Hydrogenation of Benzene on Ni(111)—A DFT Study

F. Mittendorfer*,†,‡ and J. Hafner†

Institut für Materialphysik and Center for Computational Materials Science Universität Wien, Sensengasse. 8/12, A-1090 Vienna, Austria, and Institut Français du Pétrole, 1&4 Avenue de Bois-Préau, 92852 Rueil-Malmaison, France

Received: April 24, 2002; In Final Form: October 4, 2002

The hydrogenation of benzene to cyclohexadiene on a Ni(111) surface has been studied using ab-initio local-density-functional calculations. The calculations were performed using the Vienna ab-initio simulation package (VASP), which is based on a plane wave basis set and PAW potentials. Starting from benzene preadsorbed on the nickel surface reaction pathways for the hydrogenation of the benzene molecule to cyclohexadiene by a Langmuir−Hinshelwood mechanism have been investigated. In the optimized reaction path, the initial step is a dissociation of the hydrogen molecule over a nickel surface atom. The rate-determining step has been identified as the first hydrogenation step, i.e., the formation of C_6H_7, with an energetic barrier of 0.7 eV. Parallel to that, the direct interaction of the hydrogen molecule with the adsorbed molecule in an Eley−Rideal reaction has been studied. The Eley−Rideal reaction leads to a much higher barrier. A detailed analysis of the structural and electronic properties of the molecule at the corresponding transition states is presented.

1. Introduction

The hydrogenation of benzene is not only a model system for the hydrogenation of aromatic compounds, but also a fundamental process for the refining industry as environmental restrictions limit the benzene content of gasoline. As a result, processes for the reduction of the concentration of aromatics in fuels have received considerable attention in the recent years.

Most of the commercial hydrotreating catalysts based on sulfides of Co−Mo, Ni−Mo, and Ni−W supported on γ-alumina require high temperatures and hydrogen partial pressures due to their poor activity. Catalysts based on supported group VIII metals such as Pt, Pd, Ru, and Ni could significantly improve the efficiency of these processes,[1] although their sensitivity for sulfur poisoning might restrict their commercial use in processing sulfur-containing feedstock.

Even though heterogeneous hydrogenation of benzene over supported and unsupported Ni catalysts has been well studied for some time,[1−10] fundamental aspects of the reaction kinetics are still unresolved. The reported activation energies range from 25 to 94 kJ mol^{-1} (0.26−0.97 eV); the reaction order with respect to benzene is given in a range from 0 to 0.5, with respect to the hydrogen partial pressure from 0.5 to 3.[2]

Ab-initio calculations offer a direct access to the properties such as the reaction barriers determining the reaction kinetics that are not directly accessible with experimental tools. Although many of the industrial metal catalysts are based on supported metals, this study is dedicated to the investigation of the catalytic properties of a pure metal surface. While the adsorption of benzene on transition metal surfaces has been discussed in several recent density functional theory (DFT) studies,[11−14] much less is known about reactions of aromatic molecules on these surfaces from a theoretic point of view. Therefore, the ab-initio study of a model system, the hydrogenation of benzene to cyclohexadiene over a Ni(111) surface, is presented.

2. Methodology

Computational Setup. The calculations were performed using the Vienna ab-initio simulation package (VASP).[15,16] VASP performs an iterative solution of the Kohn−Sham equations of the density functional theory (DFT) using residuum-minimization techniques and optimized charge-density mixing routines. The program uses a plane-wave basis set, offering thus a good access to the Hellmann−Feynman forces acting on the atoms. The calculations were performed using the projector-augmented wave (PAW) method[17,18] and generalized gradient (GGA) corrections as proposed by Perdew et al.[19] For the plane wave set, a cutoff energy of 400 eV was used.

The Brillouin-zone integrations have been performed using a $4 \times 4 \times 1$ Monkhorst-Pack grid[20] and a Methfessel-Paxton smearing[21] of 0.1 eV. The calculations were performed for a nonmagnetic substrate. The influence of the magnetism has been found to lower the adsorption energies of benzene adsorbed on Ni(111).[11] Therefore, the main reaction barrier has been considered additionally in a fully relaxed spin-polarized calculation, but the change of the energetic barrier due to the substrate magnetism has been found to be less than 30 meV.

The structure of the supercell was determined by the experimental $\sqrt{7} \times \sqrt{7}$ $R19.1°$ superstructure formed by the benzene molecules at saturation coverage, and the surface was modeled by a four-layer slab with the uppermost layer allowed to relax.

The transition states of the reaction were determined using the Nudge-Elastic-Band Method.[22] This method is based on an explicit mapping of the minimum-energy-path connecting two local minima via a simultaneous calculation of a series of replica, the images. These images are allowed to relax in a hyperplane perpendicular to the reaction coordinate, thus converging to points along the minimum energy path. In the chemical interpretation, the initial state of the system corresponds to the

* Corresponding author. E-mail: Florian.Mittendorfer@ifp/fr.
† Institut für Materialphysik and Center for Computational Materials Science Universität Wien.
‡ Institut Français du Pétrol.

10.1021/jp026010z CCC: $22.00
Published on Web 12/02/2002

TABLE 1: Energy Gain ($\Delta E = E_B + xE_B(H_2) - E_B(C_6H_{12})$) of Benzene ($C_6H_6$), the Isomers of Cyclohexadiene (C_6H_8), and Cyclohexene (C_6H_{10}) on Hydrogenation to Cyclohexane (C_6H_{12}) Calculated with the PW91, the PBE, and the Meta-GGA Exchange-Correlation Functional

ΔE_B [eV]	PW91	PBE	meta-GGA	exp.[26]
benzene	2.79	2.79	1.96	2.13
1,3-cyclohexadiene	2.89	2.89	2.35	2.37
1,4-cyclohexadiene	2.91	2.91	2.39	
cyclohexene	1.49	1.48	1.22	1.23

reactants, the final state to the products of the reaction, and the connecting minimum energy path to the reaction pathway. The transition states have been obtained by a further relaxation of the image closest to the barrier, using a quasi-Newton algorithm. In addition, the transition states have been verified by the calculation of the vibrational frequencies within an harmonic approach. For the presented calculations, up to 16 images per reaction step have been used; however, only the transition states will be discussed in detail.

Choice of the Exchange-Correlation Functional. The energy gain for the separate steps of the hydrogenation has a crucial impact on the reaction mechanisms. Although density-functional calculations with the Perdew-Wang 91 (PW91) exchange-correlation functional[19] and its reformulation by Perdew, Burke, and Ernzerhof (PBE)[23] offer an accurate description of the structural properties of molecules, the accuracy of binding energies of gas-phase molecules has been problematic for several cases. Especially new approaches such as the use of a meta-GGA functional[24,25] (based on the local kinetic energy density) claim to allow a more precise description. Hence the difference in the binding energies of the molecules has been determined using several functionals; Table 1 gives the energy-gain of the gas-phase intermediates through the hydrogenation to cyclohexane:

$$\Delta E = E_B(C_6H_{12-2x}) + xE_B(H_2) - E_B(C_6H_{12})$$

with the binding energy $E_B(C_6H_{12-2x}, x = 1,2,3)$ of the molecule, $E_B(C_6H_{12})$ of cyclohexane, and the binding energy $E_B(H_2)$ of a hydrogen molecule multiplied with the number of H_2 molecules needed to fulfill the stoichiometry.

The Perdew-Wang 91 (PW91) results give the trends in the energetics of the crucial steps. Generally, each hydrogenation step leads to an increase of the binding energy. Still the energy gain for the hydrogenation of cyclohexadiene is larger than the gain for benzene, as the first step, the hydrogenation of benzene to cyclohexadiene, is an endothermic process due to the aromatic stabilization of benzene.

For 1,4-cyclohexadiene, the PW91 calculations predict bond lengths of 1.34 Å for the double bonds and 1.50 Å for the single bonds in comparison to experimental values of 1.35 Å and 1.51 Å.[27]

For 1,3-cyclohexadiene, a value of 1.35 Å (exp.: 1.35 Å[28]) has been determined for the length of the double bond. A bond length of 1.46 Å (exp.: 1.47 Å[28]) has been calculated for the single bond located between atoms 2 and 3 (the 2−3-bond), a value of 1.51 Å (exp.: 1.52 Å[28]) for the 4−5-bond, and a value of 1.54 Å (exp.: 1.54 Å[28]) for the 5−6-bond.

In the case of cyclohexene, the calculations predict a value of 1.34 Å (exp.: 1.34 Å[29]) for the double bond, a value of 1.51 Å (exp.: 1.51 Å[29]) for the adjoining bonds, and finally a value of 1.53 Å (exp.: 1.53 Å[29]) for the remaining three C−C bonds.

The calculations predict a value of of 1.53 Å (exp.: 1.54 Å[30]) for the C−C bondlengths of cyclohexane.

TABLE 2: Structural and Energetic Parameters of Benzene/Ni(111) Hydrogenated to Cyclohexadiene: Adsorption Energy E_{Ads} As Described in the Text, C−C Distances D(C−C), and Angle (HCH) for 1,3- and 1,4-Cyclohexadiene (CHD), 1,3-Dihydrobenzene (DHB), and Cyclohexane

	E_{ads} [eV]	d(C−Ni)	d(C−C) [Å]	d(C−H) [Å]	C−H−C [deg]
1,3-CHD	0.06	2.01/2.07	1.46−1.53	1.10	106
1,4-CHD	0.28	2.05	1.41/1.50	1.11	105
1,3-DHB	0.13	1.99	1.44/1.52	1.10	105
cyclohexane	−1.82	3.17	1.53	1.10	106

Although the PW91 respectively the PBE functional allow a very accurate description of the structure of the molecules, the calculation of differences in the binding energies of gas-phase molecules is much less accurate.[23] Especially for the energetic difference between benzene (C_6H_6) and cyclohexane (C_6H_{12}), an error of 0.66 eV was encountered. With an error of 0.17 eV, the usage of the meta-GGA functional results in a significant improvement.

For cyclohexadiene and cyclohexene, the errors in the energetic difference with respect to cyclohexane are less dramatic in the PW91-GGA. Again, the meta-GGA functional leads to an improved description. These results indicate that the correction terms containing the kinetic energy of the valence electrons greatly improve the prediction of the energetic difference between single and double bonds.

3. Adsorption of Cyclic Hydrocarbons on Ni(111)

The results from the previous section have shown that the first step, the hydrogenation of benzene to cyclohexadiene, is especially unfavorable in the gas phase due to the fact that it is an endothermic reaction. However, the chemisorptive interaction with the metal surface leads to a rehybridization of the molecular bonds, often stabilizing molecules which would be unstable in the gas phase and thus allowing different reaction mechanisms. Hence, the adsorption of the isomers of cyclohexadiene/Ni(111) has been investigated in the following section.

Since the main interest in this study was in the hydrogenation of preadsorbed benzene, the starting position for the following calculations was the energetically most favorable adsorption geometry for benzene/Ni(111) with the molecule adsorbed over a bridge site. A detailed discussion of this system is given in ref 11.

Table 3 gives an overview of the adsorption energies (with the energy of benzene adsorbed in the bridge position and the binding energy of H_2 in the gas phase as reference energy: $E_{ads} = E(C_6H_{6+2n}/Ni(111)) - E(C_6H_6/Ni(111) + n^*E_B(H_2))$ and the structural parameters of the optimized geometries.

In contrast to the reaction in the gas phase, where the energy loss in the initial hydrogenation step is nearly identical for both isomers with values of $\Delta E_{ads} = 0.10$ eV for 1,3- and $\Delta E_{ads} = 0.12$ eV for 1,4-cyclohexadiene, on the metal surface different trends for the isomers are observed. For the energetically most favored 1,3-cyclohexadiene, the energy is close to the reference energy (the energy of the preadsorbed benzene molecule plus the binding energy of a H_2 molecule). Hence, the first hydrogenation step is less endothermic than in the gas phase, whereas the hydrogenation to 1,4-cyclohexadiene on Ni(111) has an even higher energetic cost than for the gas-phase molecules. 1,3-Dihydrobenzene, a molecule which would be unstable in the gas phase, is stabilized by the bonds to the substrate.

Figure 1 displays the optimized adsorption geometries of the isomers. In the case of the adsorption of 1,3-dihydrobenzene

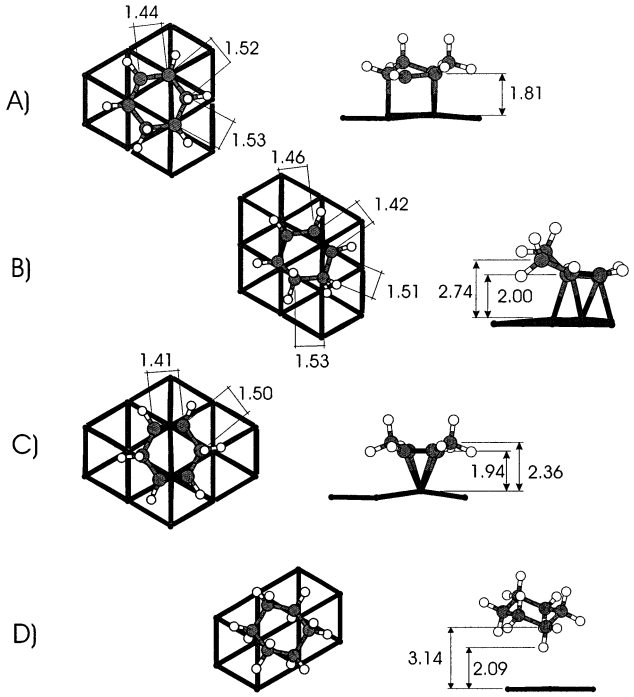

Figure 1. Structure of benzene adsorbed on Ni(111) after the hydrogenation to (A) 1,3-dihydrobenzene, (B) 1,3- and (C) 1,4-cyclohexadiene, and (D) cyclohexane. C−C bonds corresponding to double bonds in the gas phase are marked by darker shading.

(Figure 1A), the molecule drifts from the bridge to the hollow site. The bonds of the hydrogenated carbon atoms to the Ni substrate are broken, the intramolecular carbon−carbon distances are expanded to a bond length of 1.52 Å respectively 1.44 Å as a result of the decreasing bond strength.

After the adsorption on the Ni surface, 1,3-cyclohexadiene (Figure 1B) is found to be the energetically most favorable isomer. The ring adsorbs with the double bonds parallel to the surface, while the hydrogenated carbon atoms are tilted away from the surface. The bond length of the double bonds increases from a value of 1.35 Å for the free molecule to a value of 1.42 Å, the remaining bonds show the same bond length as in the gas phase, which confirms the assumption that the adsorption is dominated by the interaction between the π-orbitals forming the double bond and the metal surface, as described for the adsorption of benzene.[11]

A similar adsorption mechanism is found for the adsorption of 1,4-cyclohexadiene (Figure 1 C). The bond length of the two double-bonds is increased from a value of 1.34 Å in the gas phase to a value of 1.41 Å for the adsorbed species, again stressing the importance of the former double bonds for the interaction, whereas the values of the single bonds remain unchanged. The two double bonds are oriented parallel to the surface, whereas the hydrogenated carbon atoms are tilted away.

The number of chemisorptive bonds to the surface is reduced with each hydrogenation step, after the hydrogenation to cyclohexane (Figure 1D) the molecule is only physisorbed to the surface in its gas-phase structure with a distance of $\Delta d_z(\mathrm{H}) = 2.09$ Å respectively $\Delta d_z(\mathrm{C}) = 3.14$ Å between the Ni surface and the closest hydrogen respectively carbon atom. Although cyclohexane is physisorbed on the surface, the interaction is strong enough to cause a considerable shift in the vibrational modes involving C−H bonds oriented toward the surface; while in the gas phase, the calculated C−H stretching frequencies are found in a range from 2948 to 3010 cm^{-1}, frequencies are shifted to a range of 2725−3035 cm^{-1} for the adsorbed case. This shift is in reasonable agreement with EELS experiments performed by Demuth et al.[31] who report the formation of a broad second CH-peak centered at 2720 cm^{-1}.

4. Hydrogenation of Adsorbed Benzene

4.1. Reaction Path A: Langmuir−Hinshelwood-type Mechanism. *4.1.1. Reaction Pathway*. Although the issue of the reaction order for the hydrogenation of benzene over a nickel catalyst is still not solved, most experiments agree that it is close to zero at low temperatures and high partial pressures of the aromatic compound.[2] Hence, the hydrogenation process of benzene/Ni(111) to 1,3-cyclohexadiene/Ni(111) has been investigated starting from preadsorbed benzene at the saturation coverage.

Although several reaction pathways following a Langmuir−Hinshelwood type mechanism could be considered, the shortest pathway has been investigated in detail. The NEB calculations were performed starting from a linear interpolation between the structures of the reaction intermediates. Figure 2 gives the geometric configuration of intermediates and transition states and the energetic profile along the reaction path.

The initial reaction step is the dissociation of the hydrogen molecule over a vacant top site of the Ni substrate. Although the dissociative adsorption of H_2 has next to no barrier on the clean Ni(111) surface,[33] the energetic barrier rises as a result of the high coverage of the coadsorbed benzene molecules to a value of 0.47 eV with an imaginary frequency of 402 cm^{-1} (II-transition state 1). After the dissociation, the hydrogen atoms are located in neighboring hollow sites, which are also favored for the adsorption of H on a clean Ni(111) surface, forming the first reaction intermediate (III).

The following reaction step is the first hydrogenation of the benzene molecule: after overcoming an activation barrier of 0.73 eV (configuration IV—transition state 2 with an imaginary frequency of 500 cm^{-1}) one of the carbon atoms is hydrogenated, which causes a slight rotation of the molecule (C_6H_7) in the second intermediate state (V). After the second hydrogenation step (VI) with a lower activation energy of 0.40 eV and an imaginary frequency of 982 cm^{-1} the benzene molecule is hydrogenated to 1,3-cyclohexadiene adsorbed on the Ni surface (VII). Although the hydrogenation of benzene to cyclohexadiene is an endothermic process in the gas phase, this energetic difference is decreased to a value of only 0.06 eV for the adsorbed benzene molecule.

The complete hydrogenation of the molecule to cyclohexane results in a total energy gain of 1.93 eV. As discussed in the previous section the hydrogenation weakens the bonds to the substrate which results in a mere physisorption of cyclohexane, which thus facilitates its desorption, closing the catalytic cycle.

Figure 3 gives the detailed structural properties of the transition states. The first transition state (A) is determined by the dissociation of the hydrogen molecule. With distances of $d(\mathrm{H-Ni}) = 1.51$ Å respectively 1.64 Å the interaction between the hydrogen atoms and the substrate molecule is already strong enough to allow the elongation of the H−H bond from the gas-phase value of $d(\mathrm{H-H}) = 0.75$ Å to a value of $d(\mathrm{H-H}) = 1.04$ Å. After the dissociation, the atoms are located in the hollow sites of the surface.

At the second transition step (B), the initial hydrogenation takes place. The hydrogen atom is located at a hollow site, the benzene molecule is slightly rotated. This rotation stretches the distance between the hydrogenated carbon atom and the Ni substrate atom to a value of $d(\mathrm{C-Ni}) = 2.27$ Å, weakening the interaction with the substrate and thus favoring the formation

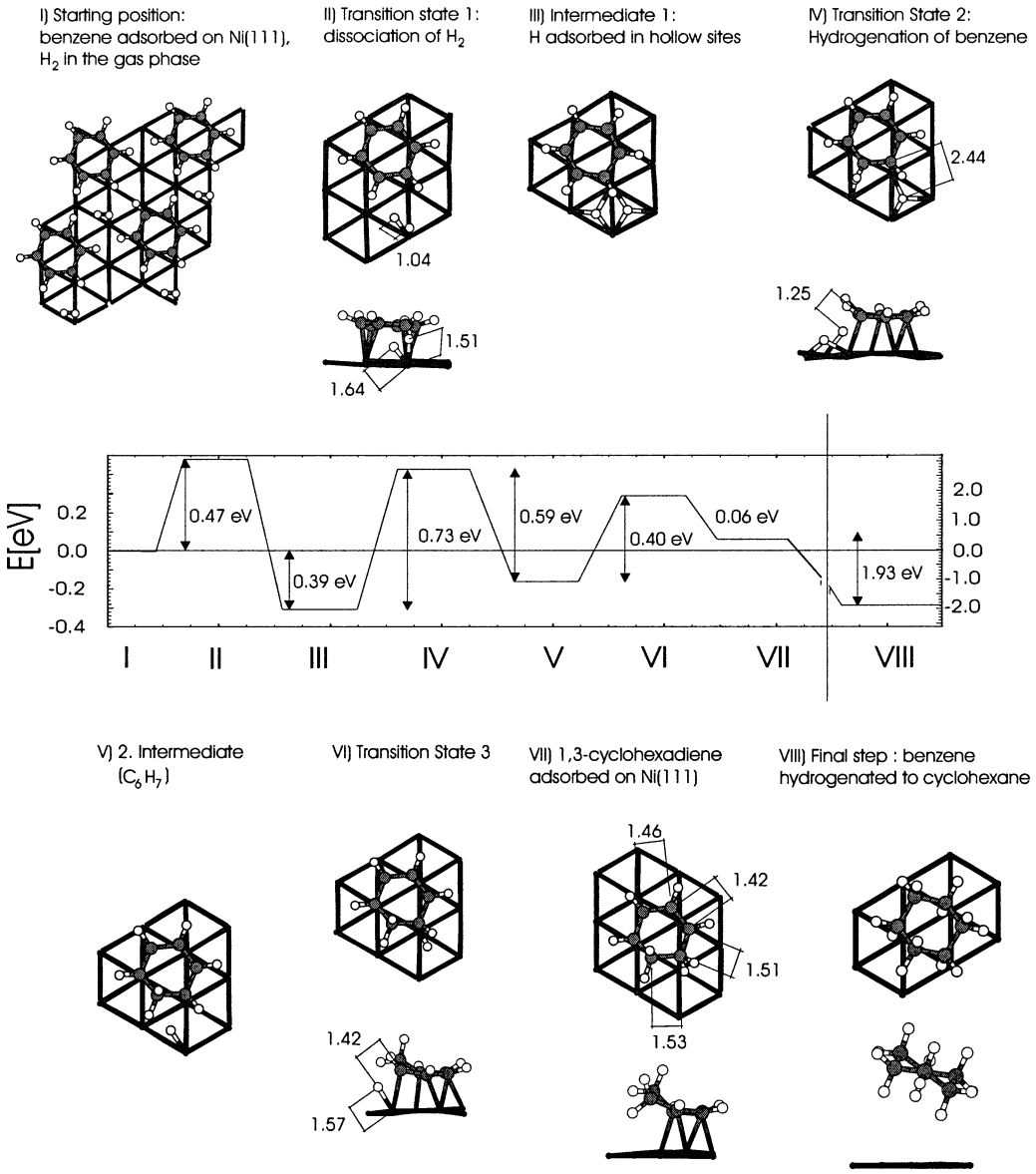

Figure 2. Energy profile of the hydrogenation of benzene adsorbed on Ni(111) according to a Langmuir−Hinshelwood mechanism. Starting from preadsorbed benzene/Ni(111) (I), the hydrogen molecule is dissociatively adsorbed on the surface (II), followed by a stepwise hydrogenation of the benzene molecule (IV, VI). Hydrogenated to cyclohexane (VIII), the molecule is only physisorbed on the surface.

of a new bond. The transition state is rather late as only a rather short distance between the additional hydrogen atom and the carbon atom of d(C−H) = 1.25 Å allows for a sufficiently strong interaction.

In agreement with the lower activation energy, the transition state for the second hydrogenation (C) is already reached earlier; at a distance of d(H−Ni) = 1.57 eV the second hydrogen atom is weakening the C−Ni bond through the interaction with the Ni states, while the distance to the carbon atom d(C−H) = 1.42 Å is larger than in the initial hydrogenation step.

4.1.2. Reaction Mechanism. Further insight into the reaction mechanism can be gained from an analysis of the electronic properties at the reaction steps. A comparison of the local density of states (LDOS) of the transition states of the two initial hydrogenation steps illustrates their different character.

Figure 4 shows the LDOS of the involved reactants for the initial hydrogenation (A) at the first reaction intermediate with the dissociated hydrogen atoms located in the hollow sites, (B) at the transition step, and (C) for 1,3-cyclohexadiene adsorbed on Ni(111). The transition state for the first hydrogenation step (B) is reached rather late. At this point the interaction of the hydrogen atom with the substrate is weakened compared to the initial adsorption in hollow position, but still a hybridization with the substrate d_{yz} band results in the occupation of a bonding state at an energy of −3 eV with respect to the Fermi energy, respectively an antibonding state close to the Fermi level. Moreover, this step involves already a strong interaction between the benzene molecule and the additional hydrogen atom. At a distance of d(C−H) = 1.25 Å the hydrogen s-states are hybridizing with the low-lying σ-states of the benzene molecule and carbon p_z- respectively p_y-states oriented toward the molecule. Through the starting rehybridization of the molecule, the state at a binding energy of −5 eV corresponding to a molecular orbital formed by C−H bonds is significantly broadened.

The electronic structure at the transition state for the second hydrogenation step differs in several aspects. Figure 5 shows a comparison between the first reaction intermediate, the second hydrogenation step, and the final configuration projected on the involved atoms. The transition state is reached earlier than in the previous case; due to the closer distance to the nearest Ni atom d(H−Ni) = 1.57 Å and the larger distance to the carbon

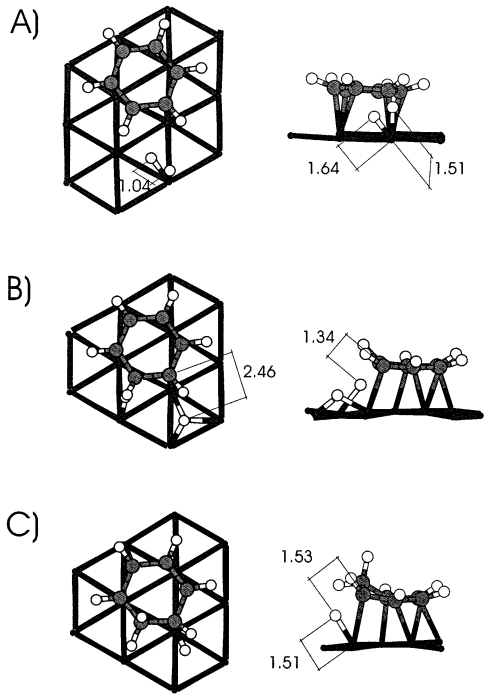

Figure 3. Geometric characterization of the transition states for the hydrogenation of benzene adsorbed on Ni(111): (A) at the initial dissociation of the hydrogen molecule over a top site, (B) at the first hydrogenation step, and C) at the second hydrogenation step. All distances are given in Å.

atom with a value of d(C−H) = 1.42 Å the hydrogen atom forms still a strong bond to the Ni substrate. In addition, this bond weakens significantly the bond between the same substrate atom and the benzene molecule, as illustrated by a lesser occupation of the Ni−C hybrid state at a binding energy of −2 eV in the LDOS of the carbon atom and an increased occupation of the Ni d-states in this region.

After the benzene molecule was hydrogenated to 1,3-cyclohexadiene/Ni(111) (C), the hydrogen atom is fully hybridized with the molecular eigenstates. The hybrid states between the carbon atom and the substrate close to the Fermi level have vanished, indicating a rupture of the carbon−nickel bonds. This observation is confirmed by an increased occupation of the Ni d-states at an binding energy of −1 eV below the Fermi level, formerly decreased by the adsorption of the benzene molecule.

4.1.3. Influence of the Choice of the Functional: PW 91 vs meta-GGA. The discussion of the molecules in the gas phase has shown a significant influence of the choice of the functional on the molecular binding energies, especially for the prediction of energetic differences between single and double bonds. However, a recent study has shown[25] that the use of the meta-GGA functional for the determination of adsorption energies of small molecules on metallic surfaces resulted only in minor corrections to energies calculated with the Perdew-Wang 91 (PW91) functional.

Kinetic considerations in the framework of the transition state theory postulate an exponential dependency of the reaction rate constant on the height of the activation energy.[32] Hence the influence of the choice of functional on the height of the reaction barriers is of central interest. Table 3 gives an overview over the reaction barriers calculated with the PW91 and the meta-GGA functionals. The labeling of the intermediates (Ix) respectively the transition states (Tx) was chosen according to Figure 2. A comparison between the barriers calculated with the PW91 functional and the meta-GGA shows that the differences are less than 60 meV for all barriers. This tendency is in agreement with the trends observed for adsorption energies on metal surfaces.[25] Consequently the use of a meta-GGA functional, while resulting in significant improvements for binding energies of gas-phase molecules, is found to have only a minor impact on the reaction barriers. This reflects the fact that due to the interaction with the substrate, the difference between a single and a double bond and between aromatic and nonaromatic behavior is considerably reduced.

4.2. Reaction Path B: Eley−Rideal-type Mechanism. Finally an alternative reaction according to an Eley−Rideal mechanism has been investigated. In the chosen reaction pathway the preadsorbed benzene molecule is directly hydrogenated from the gas phase.

Figure 6 displays the energetic profile along the reaction path. The transition state is associated with an energy barrier of 2.8 eV (imaginary frequency: 759 cm^{-1}) strongly disfavoring this mechanism. The hydrogen−hydrogen distance at the transition

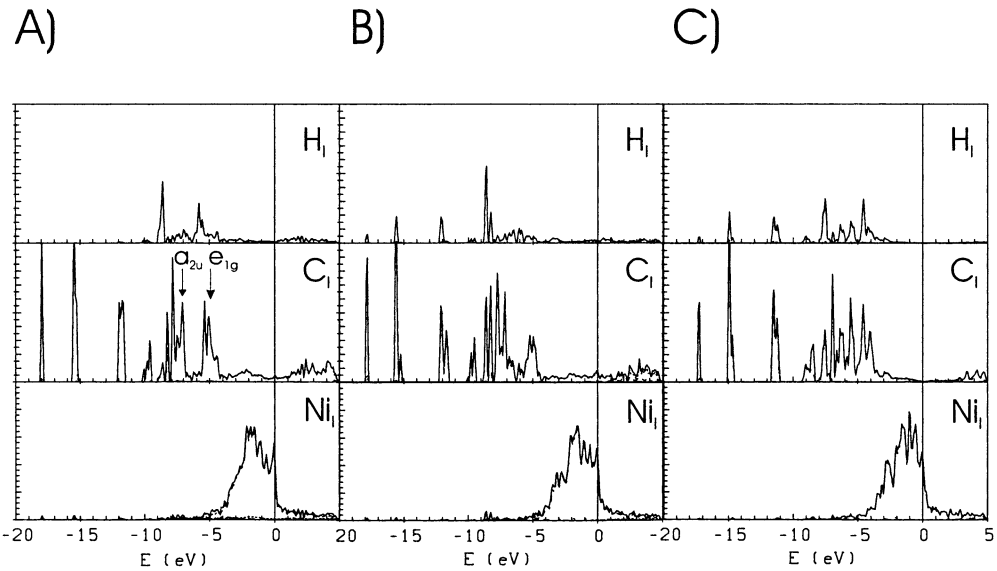

Figure 4. Comparison of the Local Density of States (LDOS) for the first hydrogenation step (A) at the first intermediate with the hydrogen atoms adsorbed in the hollow positions, (B) at the transition state, and (C) for 1,3-cyclohexadiene adsorbed on Ni(111). The DOS is displayed for the additional hydrogen atom (H), the carbon atom involved in the hydrogenation (C), and the nearest surface Ni atom (Ni).

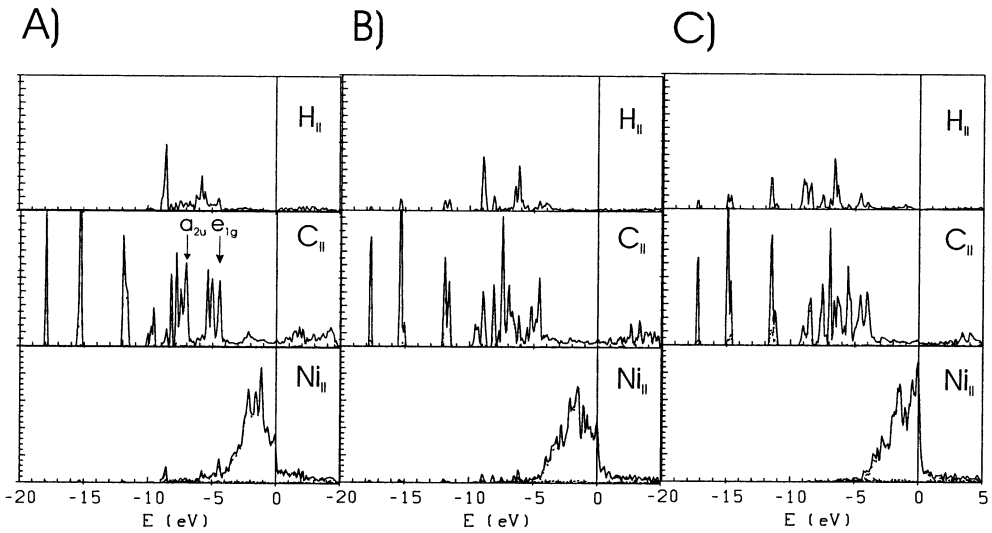

Figure 5. Comparison of the Local Density of States (LDOS) for the second hydrogenation step (A) at the first intermediate with the hydrogen atoms adsorbed in the hollow positions,)B) at the transition state, and (C) for 1,3-cyclohexadiene adsorbed on Ni(111). The DOS is displayed for the additional hydrogen atom (H), the carbon atom involved in the hydrogenation (C), and the nearest surface Ni atom (Ni).

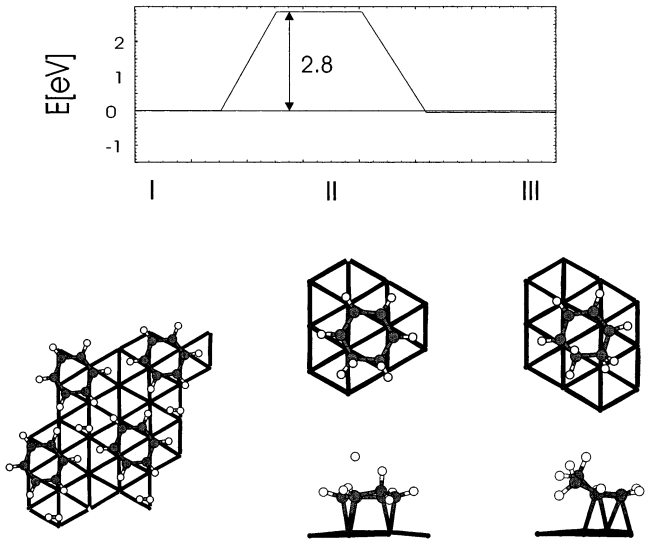

Figure 6. Reaction path for a hydrogenation of benzene to cyclohexadiene on Ni(111) according to an Eley−Rideal mechanism: starting position (I), transition state (II), and 1,3-cyclohexadiene/Ni(111).

TABLE 3: Changes in the Reaction Barriers for the Hydrogenation of Benzene to Cyclohexadiene/Ni(111) (CHD) with the Use of Different Functionals[a]

	ΔE(I1 − T2)	ΔE(I1 − T2)	ΔE(I2 − 3)	ΔE(T3 − CHD)
PW91 [eV]	0.73	−0.59	0.40	-0.17
meta-GGA [eV]	0.72	−0.63	0.34	-0.22

[a] The labeling of the reaction intermediates (I*x*) and transition states (T*x*) is according to Figure 2.

state has a value of 1.7 Å, one of the hydrogen atoms forms already bonds to the molecule. The height of the barrier allows us to exclude this reaction type from further considerations.

Conclusions

In summary, we have performed a detailed ab-initio study of the initial steps of the hydrogenation and de-aromatization of benzene catalyzed by a Ni(111) surface. The complete path for the hydrogenation of benzene to 1,3-cyclohexadiene over a Ni(111) surface has been investigated with ab-initio methods. This reaction is seen as the crucial step for the hydrogenation of benzene to cyclohexane.

We find that although the transformation of benzene to both isomers of cyclohexadiene is an endothermic reaction in the gas phase, the interaction with the surface reduces the endothermic heat of reaction for this step. This effect is stronger for 1,3-cyclohexadiene than for 1,4-cyclohexadiene. The reason is that for 1,4-cyclohexadiene the bonding is restricted to fewer substrate atoms.

A comparison of the reaction mechanisms clearly favors a Langmuir−Hinshelwood-type mechanism compared to an Eley−Rideal-type mechanism. The proposed reaction mechanism takes place in several steps. Prior to the hydrogenation, the H_2 molecule is dissociated over the top position. As a consequence of the high coverage by coadsorbed benzene, a barrier of 0.47 eV is found for this step. It is clear that at a lower coverage, this barrier will be considerably reduced. However, if H_2 dissociation takes place farther away from the benzene molecule, the diffusion of atomic H has to be considered. On Ni(111), this barrier is only 0.15 eV, according to Kresses calculations.[33] Still, even at saturation coverage, the rate-determining step for the hydrogenation is the initial hydrogenation of the molecule, which has an energetic barrier of 0.73 eV; as for the second hydrogenation step, the calculated barrier has a lower value of 0.40 eV. Therefore, taking the reaction barrier of the Eley−Rideal mechanism of adsorbed benzene with gas-phase H_2 ($\Delta E \sim 2.8$ eV) as a lower limit for a gas-phase reaction, we find that a Ni-catalyst reduces the barriers by about 2 eV.

For gas-phase molecules, the PW-91 (GGA) functional allows an accurate description of the structural parameters, yet the meta-GGA functional offers an improvement in the determination of energetic differences between single and double bonds. A comparison of the energetic barriers calculated within the PW91 respectively the meta-GGA functional shows only a minor influence of the choice of the functional.

Acknowledgment. This work has been supported by the Austrian Science Funds within the Science College "Computational Materials Science" (W004).

References and Notes

(1) Stanislaus, A.; Cooper, B. H. *Catal. Rev.—Sci. Eng.* **1994**, *36*, 75.

(2) Bond, G. C.; Keane, M. A.; Kral, H.; Lercher, J. A. *Catal. Rev.—Sci. Eng.* **2000**, *42*, 323.

(3) Keane, M. A.; Patterson, P. M. *Ind. Eng. Chem. Res.* **1999**, *38*, 1295.
(4) Dalmai-Imelik, G.; Massardier, J. In *Proceedings of the 6th International Congress on Catalysis*: London, 1976; p 90.
(5) Mirodatos, C.; Dalmon, J. A.; Martin, G. A. *J. Catal.* **1987**, *105*, 405.
(6) Germain, J. E.; Maurel, R.; Bourgeois, Y.; Sinn, R. *J. Chim. Phys.* **1963**, *60*, 1219.
(7) van Meerten, R. Z. C.; Coenen, J. W. E. *J. Catal.* **1975**, *37*, 37.
(8) Franco, H. A.; Phillips, M. J. *J. Catal.* **1980**, *63*, 346.
(9) Son, K.-A.; Gland, J. L. *J. Phys. Chem B* **1997**, *101*, 3540.
(10) Toppinen, S.; Rantakylä, T.-K.; Salmi, T.; Aittamaa, J. *Ind. Eng. Chem. Res.* **1996**, *35*, 1824.
(11) Mittendorfer, F.; Hafner, J. *Surf. Sci.* **2001**, *472*, 133.
(12) Yamagishi, S.; Jenkins, S. J.; King, D. A. *J. Chem. Phys.* **2001**, *114*, 5765.
(13) Saeys, M.; Reyniers, M.-F.; Marin, G. B.; Neurock M. *J. Phys. Chem.* **2002**, *106*, 7489.
(14) Held, G.; Braun, W.; Steinrück, H.-P.; Yamagishi, S.; Jenkins, S.; King, D. A. *Phys. Rev. Lett.* **2001**, *87*, 216102.
(15) Kresse, G.; Hafner, J. *Phys. Rev. B* **1993**, *47*, C558.
(16) Kresse, G.; Furthmüller, J. *Comput. Mater. Sci.* **1996**, *6*, 15.
(17) Blöchl, P. E. *Phys. Rev. B* **1994**, *50*, 17953.
(18) Kresse, G.; Joubert, D. *Phys. Rev. B* **1999**, *59*, 1758.
(19) Perdew, J. P.; Chevary, J. A.; Vosko, S. H.; Jackson, K. A.; Pederson, M. R.; Singh, D. J.; Fiolhais, C. *Phys. Rev. B* **1992**, *46*, 6671.
(20) Monkhorst, H. J.; Pack, J. D. *Phys. Rev. B* **1976**, *13*, 5188.
(21) Methfessel, M.; Paxton, A. *Phys. Rev. B* **1989**, *40*, 3616.
(22) Mills, G.; Jónsson, H. *Phys. Rev. Lett.* **1994**, *72*, 1124.
(23) Perdew, J. P.; Burke, K.; Ernzerhof, M. *Phys. Rev. Lett.* **1996**, *77*, 3865.
(24) Perdew, J. P.; Kurth, S.; Zupan, A.; Blaha, P. *Phys. Rev. Lett.* **1999**, *82*, 2544.
(25) Hirschl, R.; Kresse, G.; Hafner, J. To be published.
(26) Cox, J. D.; Pilcher, G. *Thermochemistry of Organic and Organometallic Compounds*; Academic Press: New York, 1970.
(27) Carreira, L. A.; Carter, R. O.; During, J. R. *J. Chem. Phys.* **1973**, *59*, 812.
(28) Oberhammer, H.; Bauer, S. H. *J. Am. Chem. Soc.* **1969**, *91*, 10.
(29) Scharpen, L. H.; Wollrab, J. E.; Ames, D. P. *J. Chem. Phys.* **1968**, *49*, 2368.
(30) Bastiansen, O.; Fernholt, L.; Seip, H. M.; Kambara, H.; Kuchitsu, K. *J. Mol. Struct.* **1973**, *18*, 163.
(31) Demuth, J. E.; Ibach, H.; Lehwald, S. *Phys. Rev. Lett.* **1977**, *40*, 1044.
(32) Eyring, H.; Daniels, F. *J. Am. Chem. Soc.* **1930**, *52*, 1472.
(33) Kresse, G. *Phys. Rev. B* **2000**, *62*, 8295.